Electroviscoelastic Effect of Polymer Blends Consisting of Silicone Elastomer and Semiconducting Polymer Particles

Tohru Shiga,* Akane Okada, and Toshio Kurauchi

Toyota Central Research & Development Laboratories, Inc., Nagakute-cho, Aichi-gun, Aichi-ken, 480-11 Japan

*Received April 19, 1993; Revised Manuscript Received September 29, 1993**

ABSTRACT: Dynamic viscoelasticity of immiscible polymer blends consisting of silicone elastomer and semiconducting polymer particles was studied under the influence of electric fields. The semiconducting polymers used experimentally were poly(*p*-phenylenes) lightly doped with $CuCl_2$ or $FeCl_3$. The dc electric fields enhanced storage and loss shear moduli of the polymer blends (electroviscoelastic effect). The ac electric fields with frequencies of less than 1 kHz also induced the electroviscoelastic effect. The electroviscoelastic effect was observed in the rubbery state of the blends with many lines of adjacent particles spanning the space between electrodes. The electroviscoelastic behavior for the polymer blends with straight lines of adjacent particles aligned to electric fields was analyzed using a point–dipole approximation model for electrically polarized particles. The presented results provide insight into the relationship between mechanical properties of the blends and the cohesive forces between electrically polarized particles.

1. Introduction

The phase morphology and the adhesion between dispersed phases in an immiscible polymer blend have been investigated extensively since they greatly affect the final performance of the blend. Recently, a new approach for the modulation of polymer blend morphology was presented by Moriya et al.[1] They demonstrated that anisotropic structures in blends could be generated by applying ac electric fields to solvent-free blends. Krause, Wnek, and co-workers also reported the use of dc electric fields to control phase morphology, especially, the shape and orientation of the dispersed phases.[2-4] The electric fields may thus open a door to the design of polymer blends having unique mechanical properties. This paper concerns the influence of electric fields on the adhesion between dispersed phases in an immiscible polymer blend.

Some kinds of suspensions of polymer particles with high dielectric constants dispersed in nonconducting oils stiffen rapidly when subjected to electric fields on the order of 1 kV/mm.[5,6] Such rheological behavior, known as the electrorheological (ER) effect, is caused by alignment of electrically polarized particles between electrodes. However, it has not been determined how the polarization of dispersed particles occurs at the molecular level although a variety of models for the polarization mechanism, including distortion of electrical double layers,[7] formation of dipoles in particles through surface charge migration, or bulk charge migration,[8] have already been proposed. If an electric field-induced dipole forms in a particle, electrical interactions always work more or less between dispersed particles which cannot move in electric fields. The interactions become strong as the dipoles get close to each other. This suggests that an interesting behavior similar to the ER effect will transpire in polymer gels or elastomers with high contents of dispersed particles. In a previous paper,[9] we first demonstrated that silicone gels containing poly(methacrylic acid) cobalt(II) salt (PMACo) particles having small amounts of adsorbed water (diameter ca. 75 μm) increased their storage and loss shear moduli at room temperature by the application of dc electric fields. The loss tangent also changed in electric fields. We called these phenomena the electroviscoelastic effect. The electroviscoelastic effect was observed in the silicone gels with high volume fractions of particles of more than 25 vol %. The samples with the electroviscoelastic capacity had many lines of adjacent particles spanning the space between electrodes before application of electric fields (Figure 1). According to our microscopic observation studies,[9] alignment of the dispersed particles by action of electric fields was not detected in the silicone gels. The electroviscoelastic effect depended on the amount of the adsorbed water in the PMACo particles. In the gels containing the PMACo particles free of water, the electroviscoelastic effect disappeared. The adsorbed water promoted ionic polarization of COO^- and Co^{2+} in the PMACo particle and enhanced the dielectric constant of the particle. The PMACo particle with a high dielectric constant produced a large electroviscoelastic effect.

Conjugated polymers such as poly(*p*-phenylene) and polythiophene can be doped from an insulating to an electrically conducting state by metal chlorides.[10] The doping increases not only the conductivity but also the dielectric constant of conjugated polymers.[10] It is, therefore, expected that the electroviscoelastic effect will be observed in gels or elastomers containing doped conjugated polymer particles. Here we report on the electroviscoelastic effect of polymer blends consisting of silicone elastomer and semiconducting polymer particles under dc or ac electric fields. In particular, we discuss the electroviscoelastic effect of polymer blends with many lines of dispersed particles aligned to electric fields theoretically as well as experimentally.

2. Theoretical Approach

The ER and electroviscoelastic effects are due to microscopic bondings between dispersed particles. However, the nature of the particle–particle forces is one of outstanding issues. It is generally thought that the ionic polarization forces (induced dipole–induced dipole interactions) are dominant, although other mechanisms have been proposed.

In ER suspensions, Klingenberg et al. first described some aspects of ER suspensions using a molecular dynamic-like simulation method (a point–dipole approximation model).[11] Real ER suspensions were modeled as monodisperse suspensions of dielectric hard spheres in a dielectric medium. The ionic polarization force of po-

* Abstract published in *Advance ACS Abstracts*, November 1, 1993.

0024-9297/93/2226-6958$04.00/0

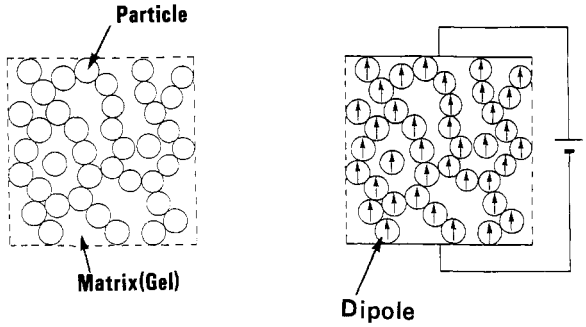

Figure 1. Schematic illustration of the electroviscoelastic effect.

larized particles was given by eq 1. where

$$F(R,\theta) = R_0\{(2r/R)^4[(3\cos^2\theta - 1)\mathbf{e}_r + \sin(2\theta)\mathbf{e}_\theta]\} \quad (1)$$

$$F_o = (3/4)\pi r^2\epsilon_0\epsilon_1\kappa^2E^2, \qquad \kappa = (\epsilon_2 - \epsilon_1)/(\epsilon_2 + 2\epsilon_1)$$

$F(R,\theta)$ is the electrostatic polarization force at a short range on sphere i at the origin of a spherical coordinate system with sphere j at $(r,\theta) = (R,\theta)$. R is the center-to-center separation between particles, and θ is the angle between the line of centers and the applied electric field. $\mathbf{e}_r$ and $\mathbf{e}_\theta$ are unit vectors in the r and θ directions, respectively. In eq 1, r is the radius of the sphere, ϵ_0 is the permittivity in vacuum ($=8.854 \times 10^{-12}$ F/m), E is the intensity of the applied fields, and ϵ_1 and ϵ_2 are the dielectric constants of the matrix and sphere, respectively. Equation 1 is obtained by solving Laplace's equation for the electrostatic potential about an isolated pair of spheres in an unbounded continuous medium.[12] Furthermore, they assumed that the spheres interacted as if they were replaced at their centers by dipoles with their magnitude equal to that induced on an isolated dielectric sphere under a uniform electric field (eq 2). Equation 2 is an expression obtained

$$\mu = 4\pi r^3\epsilon_0\epsilon_1\kappa E \quad (2)$$

formally for the volume polarizability of a particle. The net force on each sphere was calculated from the pairwise summation of the interactions with all of the other spheres. According to the point–dipole approximation model, the formation of chains induced by electric fields has been reproduced and the rheological results were qualitatively similar to the experimental results.[13,14] However, the simulated yield stress or elastic moduli were an order of magnitude smaller than the maximum that could be attained by real ER suspensions.[14]

The electrostatic forces for multibody interaction were calculated by Davis using the finite-element analysis (FEA).[15] The advantage of FEA is that an essentially exact solution is obtained that automatically includes local-field correction and multipole terms. He calculated the shear modulus for ER suspensions with chains of dielectric particles aligned along the applied electric field in a dielectric medium. The shear modulus obtained became linear at large ϵ_2/ϵ_1, for ϵ_2/ϵ_1 at least as large as 25. This result was contrary to the expectations from the point–dipole model, where it would saturate. The shear modulus of FEA was larger than that of the point–dipole model and reached the value of real ER suspensions.

The electroviscoelastic effect of our PMACo particle-filled systems has already been analyzed using the point–dipole approximation model.[16] We neglected the effect of dc conductivity because the conductivities of the PMACo particles were too small (ca. 10^{-10} S/cm). We considered a cubical blend having many straight lines of dispersed particles which remain parallel to the direction of the applied field and discussed the deformation of the cube (L, length; C, volume fraction of particle) by a shear strain from the perpendicular direction of the applied field. Macroscopic mechanical properties of the cube such as storage and loss moduli were estimated easily by multiplying the electrostatic force between adjacent particles at a short range in the line, F, by the number of the line n. The force F was calculated from eq 1 at $R = 2r$ and $\theta = 0$ (eq 3). The number of the line n was given by

$$F = (3/2)\pi r^2\epsilon_0\epsilon_1\kappa^2E^2 \quad (3)$$

$$n = \frac{\text{vol of particle in a cube}}{\text{vol of particle in one line}} = 3CL^2/2\pi r^2 \quad (4)$$

Since the electrostatic force changes the lines of dispersed particles into chains, the apparent shear modulus of the cube increases in electric fields. The obtained results suggested that the change of macroscopic mechanical properties of the PMACo particle systems was qualitatively related to the point–dipole model.

Most studies of ER suspensions and our electroviscoelastic gels have been done with dc voltages. There are many complications that may occur in electric fields, including particle charging and screening effects. The most serious one is that both the particles and the matrixes are conducting. However, the effects of conductivity have been neglected in the above discussions probably because it can be exactly unsolved. Davis attempted to analyze electrical interactions between infinitely conducting particles in an insulating medium using the FEA technique.[15] The result obtained was that the particle–particle force depended sensitively on the interparticle spacing. The force increased drastically with decreasing the spacing[17] and could be much larger than in the dielectric regime. However, it diverges when the particles touch, although the particles perhaps contact each other in chains of real ER suspensions. Thus, the effects of conductivity on the ER and electroviscoelastic effects cannot be explained perfectly until now. In this paper, we examine the electroviscoelastic effect of silicone elastomers having lightly doped conjugated polymer particles with conductivities of 10^{-10}–10^{-7} S/cm. Since the magnitudes of the conductivities are comparable with those of dispersed particles in real ER suspensions, we neglect the effects of conductivity and attempt to analyze the electroviscoelastic behavior of the polymer blends using the point–dipole approximation model at a short range. In the point–dipole model, the most important factor is the dielectric constant of a dispersed particle. So we focus on the effect of the dielectric constant of the particle on the electroviscoelastic behavior.

3. Experimental Section

Preparation of PPP. The semiconducting conjugated polymers used experimentally were poly(*p*-phenylenes) (PPPs) lightly doped with $CuCl_2$ or $FeCl_3$. $CuCl_2$ and $FeCl_3$ work against PPP as weak and strong accepters, respectively.

PPP was prepared by oxidative coupling of benzene using $CuCl_2$ and $AlCl_3$.[18] The materials were provided by Wako Chemical Ltd. In a 1-L flask, 450 g of benzene was polymerized with 385 g of $AlCl_3$, 387 g of $CuCl_2$, and 2 mL of distilled water as an initiator at 50 °C for 10 h in a nitrogen atmosphere. The products given as PPP particles were washed several times with 2 N HCl at 70 °C and dried at 150 °C for 10 h. The yield was 60 g. The residuals of Cu and Al in the particles were 0.01 wt % and 0.21 wt %, respectively, on inductively coupled plasma atomic emission spectrometry (Shimadzu Ltd. ICP-2000). The diameter of the

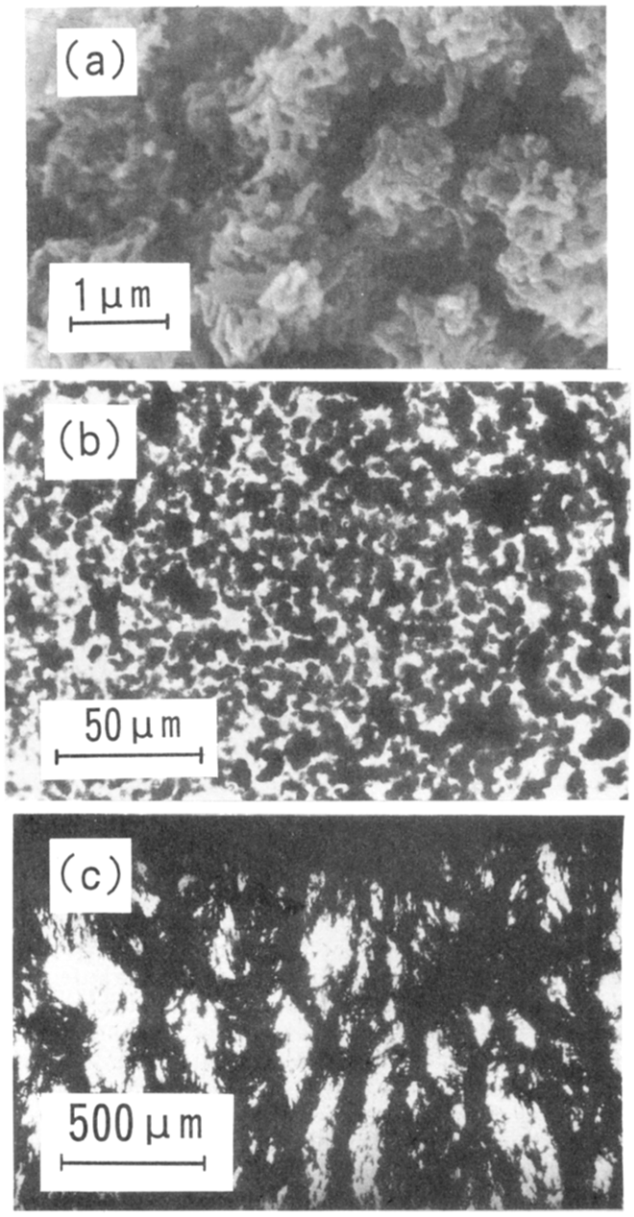

Figure 2. (a) SEM photograph of PPP particles; (b) optical photograph of PPP particles dispersed at random in the blend; (c) optical photograph of straight lines of PPP particles in the blend prepared under the influence of electric fields. The volume fraction of the particle in both b and c is 10.8 vol %.

Table I. Electrical Properties of PPP–$CuCl_2$ Particles

no.	[Cu][a]/(wt %)	σ[b]/(S cm^{-1})	ϵ_2'[c]
1	0.01	6.1×10^{-13}	6.7
2	0.12	4.2×10^{-10}	10.5
3	0.21	7.8×10^{-9}	18.8
4	0.38	1.6×10^{-8}	36.8
5	0.51	8.2×10^{-8}	68.2

[a] Cu content in the particles. [b] dc conductivity. [c] The real part of the dielectric constant at 1 kHz.

PPP particle was found to be approximately 1 μm by means of a scanning electron micrograph (Figure 2a).

Doping of Metal Chloride. The doping of $CuCl_2$ or $FeCl_3$ to the PPP particles prepared was carried out by suspending 2.5 g of the PPP particle in 100 mL of metal chloride–ethanol solutions up to 4 g/L at 60 °C. After filtration, the PPP particles suspended were dried under vacuum at 150 °C for 10 h. The Cu contents in the $CuCl_2$-doped PPP particles are listed in Table I. Table II indicates the Fe contents in the $FeCl_3$-doped PPP particles.

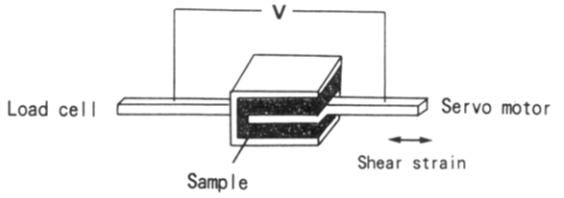

Figure 3. Schematic illustration of a test apparatus for shear viscoelastic measurement.

Table II. Electrical Properties of PPP–$FeCl_3$ Particles

no.	[Fe]/(wt %)	σ/(S cm^{-1})	ϵ_2'
6	0.11	3.8×10^{-9}	33
7	0.25	2.2×10^{-7}	128

Measurement of Electrical Properties of the Particle. The measurements of dc conductivity σ and the real part of dielectric constant ϵ_2' of the PPP particles were made using a compressed pellet of the PPP particles (10 mm in diameter and 1 mm in thickness). After upper and lower faces of the pellet were coated with Ag paste (Fuzikura Kasei Ltd., Dotite D-550), dc voltages of 10 V to 1 kV were applied between the two faces to give σ. The measurement of ϵ_2' was performed on an impedance analyzer (Hewlett Packard Ltd. 4192A). The resistance R and capacitance C of the same compressed pellet were measured by applying ac voltages of 10 Hz to 1 MHz with an amplitude of 1 V. The value of ϵ_2' was calculated from the assumption that the pellet was expressed in terms of a parallel series of R and C.

Measurement of X-ray Diffraction. X-ray diffraction patterns of PPP particles were measured at room temperature in a 2θ range between 3° and 50° using a Rigaku X-ray diffractometer (RAD-2B).

Preparation of Polymer Blends. Polymer blends of the PPP particles dispersed at random were prepared by a powder mixing method since the PPP particles were infusible and insoluble in any organic solvent. The PPP particles (0–2.5 g) were mixed with 10 g of a prereaction solution of silicone elastomer (Toray Silicone, Dow Corning Co., Ltd., SE1740). The prereaction solution mixed with the PPP particles was molded between two glass plates separated by 0.03 or 1 mm and then heated at 70 °C for 10 h to give samples. The blend films with a thickness of 0.03 mm were used as samples for microscopic observation of dispersion of the particle.

Polymer blends with many lines of the PPP particles aligned to the unidirection (see Figure 2c) were prepared as follows: First, 1.2 g of the PPP particles (no. 4 or no. 7 in Table I) was dispersed in 10 g of the prereaction solution. The mixed solution was sandwiched between two Au deposited polyester films (gap 1 mm). Next a dc voltage of 1 kV was applied across the two films, and then the mixed solution was heated at 70 °C under the applied voltage to give the blends.

Measurement of Viscoelasticity. The experiments were performed on a viscoelastic spectrometer (Iwamoto Seisakuzyo Ltd. VES-F). Figure 3 shows a schematic illustration of a test apparatus for shear viscoelastic measurements. The sample was sandwiched between an inner plate (size 8 × 8 mm) and two outer plates (gap between the inner and outer plates 1 mm). The test apparatus was set in a chamber of the viscoelastic spectrometer. The inner plate and the outer ones were connected to a servo motor and to a load cell, respectively. dc voltages up to 5 kV or ac voltages $V = V_0 \sin 2\pi ft$ ($=V_0$, 400 V; f, 0.01 Hz to 1 kHz) were applied between the outer and inner plates. The blends with many lines of particles were placed in the test apparatus so as to arrange the lines along the electric fields. The inner plate was vibrated by sinusoidally varying strains $\gamma = \gamma_0 \sin 2\pi ft$ (γ_0, 0.06; f, 10 Hz). Torque acting on the two outer plates was measured in a temperature range from −80 to +140 °C through the load cell. Shear storage and loss moduli G' and G'' and loss tangent tan δ of the blends were calculated automatically by a personal computer. The temperature dependences of the mechanical parameters were measured by heating the chamber at a rate of 2 °C/min.

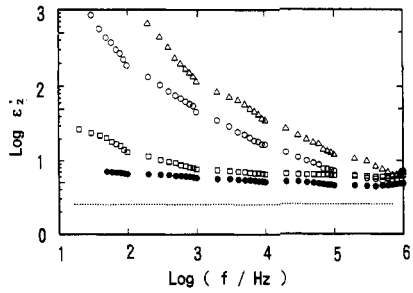

Figure 4. Frequency dependences of the dielectric constant for PPP particles: (●) no. 1; (□) no. 2; (○) no. 4; (△) no. 7. The dotted line represents the dielectric constant of the silicone elastomer.

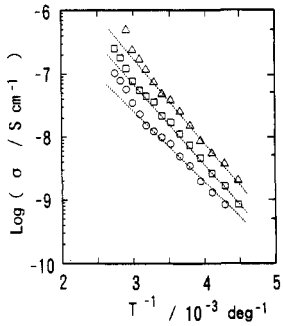

Figure 5. Temperature dependences of the dc conductivity of PPP particle no. 4. The experiments were made by applying electric fields: (○) 10 V/mm, (□) 100 V/mm, and (△) 1 kV/mm.

4. Results and Discussion

Electrical Properties of PPP Particles. Figure 4 indicates frequency dependences of the dielectric constant for PPP particles. The dielectric constant of the particle free of metal chloride (no. 1) is almost independent of frequency. On the other hand, the PPP particles containing $CuCl_2$ or $FeCl_3$ show a drastic change that the dielectric constant increases with decreasing frequency of the applied field. The content of metal chloride also influences the dielectric constant. In Figure 4, the dotted line represents the dielectric constant of the silicone elastomer as a matrix of the blends. In all the PPP particles, the dielectric constants are larger than that of the silicone elastomer.

The PPP particles containing $CuCl_2$ or $FeCl_3$ have dc conductivities of 10^{-10}–10^{-7} S/cm. They are lightly doped PPP particles since the undoped PPP particle (no. 1) has a conductivity of 6.1×10^{-13} S/cm. As shown in Tables I and II, $FeCl_3$ stands first for the doping capacity. The conductivity is strongly influenced by the content of metal chloride in the PPP particle. The conductivities of lightly doped PPP particles have not changed in air for at least 2 months. The conductivities are plotted as functions of temperature in Figure 5. The conductivity varies with the intensity of the applied field. The activation energies obtained from each slope of the σ–$(1/T)$ curve are 0.45 eV (10 V/mm), 0.48 eV (100 V/mm), and 0.53 eV (1 kV/mm). Although the extent of the doping is very light, these conductivities will probably not be due simply to metal and chloride ions.

To understand an interaction between PPP and metal chloride, we made X-ray diffraction measurements. Parts a–c of Figure 6 indicate X-ray diffraction patterns of $CuCl_2$, PPP particle no. 1, and PPP particle no. 5, respectively. There is a new X-ray peak at $2\theta = 18.6°$ in the doped PPP particle (no. 5), probably suggesting an interaction between PPP and $CuCl_2$. The peak at $2\theta = 18.6°$ has been observed in PPP particles nos. 4 and 5. The Cu content has tended to intensify the peak. The new peak has not been detected in the $FeCl_3$-doped particles because the extent of the doping was very light.

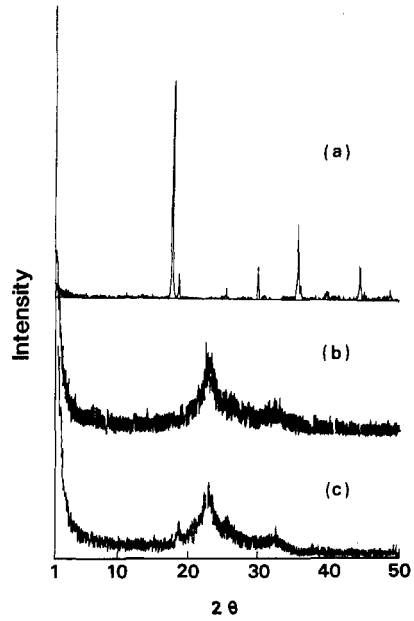

Figure 6. X-ray diffraction spectra of $CuCl_2$ (a), the undoped PPP particle (no. 1) (b), and the $CuCl_2$-doped PPP particle (no. 5) (c).

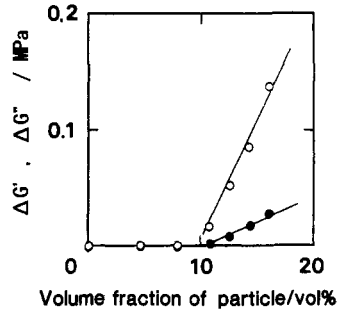

Figure 7. Effect of the volume fraction of the PPP particle on the electroviscoelastic effect. $\Delta G'$ (○) and $\Delta G''$ (●) represent the increments of the storage modulus and of the loss modulus induced by an electric field of 5 kV/mm at room temperature. The experiments were carried out using the blends of PPP particle no. 4 dispersed at random.

Electroviscoelastic Effect of Polymer Blends. Effect of the Particle Content. In order to examine whether polymer blends composed of semiconducting polymer particles show the electroviscoelastic effect, we first measured viscoelasticity of the blends with various volume fractions of PPP particle no. 4 in Table I. Figure 7 indicates the increments of G' and of G'' induced by an electric field of 5 kV/mm ($\Delta G'$ and $\Delta G''$). The electric field enhances both moduli of the blends with the particle content over 10.8 vol %. In other words, the electroviscoelastic effect has been observed in polymer blends composed of semiconducting polymer particles. Figure 2b shows an optical photograph of the PPP particles dispersed at random in the blend of 10.8 vol %. Almost all of the particles have contacted each other before application of electric fields and have formed many winding lines of dispersed particles spanning the space between electrodes. The blends with a particle content of less than 8.4 vol % could not produce the electroviscoelastic effect because they had no lines of dispersed particles. In Figure 7, the electroviscoelastic effect reflects more strongly on the storage modulus than on the loss modulus. $\Delta G'$ and $\Delta G''$ are proportional to the volume fraction.

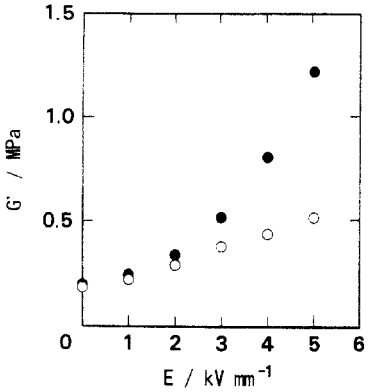

Figure 8. Effect of the dispersion of particles in polymer blends on the electroviscoelastic effect: (○) random dispersion (Figure 2b), and (●) straight lines structure (Figure 2c). In Figures 8–12 and 14, the volume fraction of the particle in all samples is 10.8 vol %.

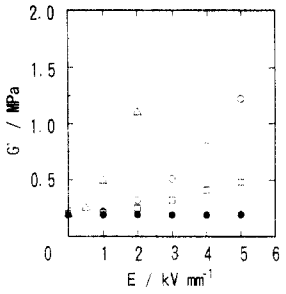

Figure 9. Electroviscoelastic effects of polymer blends of various PPP particles: (●) no. 1; (□) no. 2; (○) no. 4; (△) no. 7. In Figures 9–12 and 14, the experiments were carried out using blends with straight lines of particles.

Effect of Particle Dispersion. Figure 2c indicates an optical photograph for dispersion of particles in polymer blends prepared under the influence of electric fields. A unique structure, straight lines of PPP particles, has been observed. In Figure 8 is displayed the effect of particle dispersion on the electroviscoelastic effect. The straight lines of particles aligned to electric fields are more effective compared to the winding lines of adjacent particles in order to design a large electroviscoelastic effect.

The effect of kinds of dopants on the electroviscoelastic effect is shown in Figure 9. The experiments were carried out using polymer blends with many straight lines of particles. The $FeCl_3$-doped particle system ranks first among the blends for the electroviscoelastic capacity. The blend containing the undoped PPP particles (no. 1) has formed the straight lines in its preparation, but it shows no electroviscoelastic effect. The electrostatic forces between particles may probably be too small to yield the electroviscoelastic effect. Compared with the data in Figures 4 and 9, a high dielectric constant leads to a large electroviscoelastic effect.

Effect of the Dielectric Constant of the Particle. Equation 3 says that the electrostatic force between dispersed particles depends strongly on the dielectric constant of the particle. The force increases with ϵ_2 and approaches a constant value since κ^2 saturates ($\kappa^2 \rightarrow 1$). It is, therefore, expected that the electroviscoelastic effect may be associated with the dielectric constant of the particle. Since the dielectric constant of the particle is greatly affected by the frequency of the applied field as shown in Figure 4, we have first investigated the relationship between the electroviscoelastic effect induced by ac excitation and the frequency of the applied field. Figure 10 indicates the electroviscoelastic effect of the $FeCl_3$-doped particles-filled blend under ac excitation of 0.01 Hz

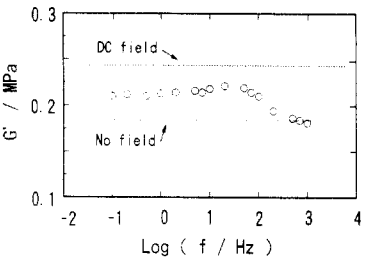

Figure 10. Electroviscoelastic effect induced by ac excitation of 0.4 V/mm. The horizontal axis represents the frequency of applied fields. The sample used was the blend of $FeCl_3$-doped PPP particles (no. 7).

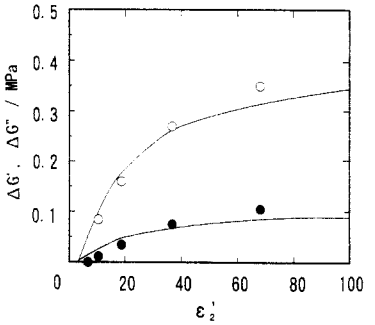

Figure 11. Relationship between the dielectric constant of the PPP particle and the electroviscoelastic effect. $\Delta G'$ and $\Delta G''$ denote the increments of storage and of loss moduli induced by a dc field of 3 kV/mm. They are plotted as functions of the real part of the dielectric constant ϵ' at 1 kHz. The solid lines represent $\Delta G' = 0.4\kappa^2$ and $\Delta G'' = 0.1\kappa^2$, respectively. Here $\kappa^2 = \{(\epsilon_2' - 2.7)/(\epsilon_2' + 5.4)\}^2$. In Figures 11–14, the PPP particle used was no. 4.

to 1 kHz. The electroviscoelastic effect maintains in the frequency range between 0.01 and 50 Hz. However, it decreases with increasing frequency of the applied field beyond 50 Hz. As the dielectric constants of the PPP particle and of the silicone elastomer at 50 Hz are 420 and 2.7, respectively, the electroviscoelastic effect induced by ac excitation of less than 50 Hz becomes constant if it follows the point–dipole model. The result obtained qualitatively corresponds to the prediction from the point–dipole model. The picture of the decrease near 50 Hz can also be explained by the model because the dielectric constant of the PPP particle decreases with increasing frequency. The electroviscoelastic effect has not been detected at frequencies over 1 kHz. These results suggest that the electroviscoelastic effect occurs through ionic polarization of the particle.

As shown in Figure 10, the electroviscoelastic effect decreases in going from dc to ac excitation. That may possibly be caused by the decrease of the field intensity as the effective value of ac excitation is given by multiplying $1/\sqrt{2}$ by amplitude. In order to clarify the relationship between the electroviscoelastic effect of dc excitation and the dielectric properties of particles, we next examined the effect of the dielectric constant of the particle on the electroviscoelastic effect in detail. The experiments were carried out using blends of $CuCl_2$-doped PPP particles. Figure 11 shows the relationship between the increments of G' and of G'' induced by a dc electric field of 3 kV/mm and the real part of the dielectric constant of the PPP particle at 1 kHz. In Figure 11, the solid lines represent $\Delta G' = 0.4\kappa^2$ and $\Delta G'' = 0.1\kappa^2$, respectively. On calculating κ, the dielectric constants of the PPP particles and the silicone elastomer ($\epsilon_1' = 2.7$) at 1 kHz were used. The experimental results are roughly related to κ^2, although they may not necessarily be correct at relatively low dielectric constants.

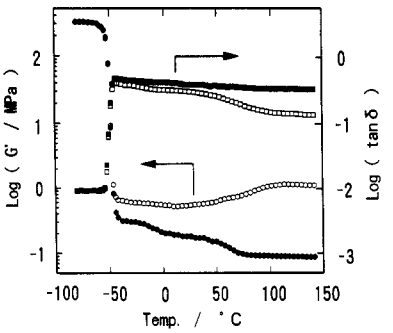

Figure 12. Temperature dependences of G' and of tan δ in electric fields of 0 (●, ■), and 3 kV/mm (○, □).

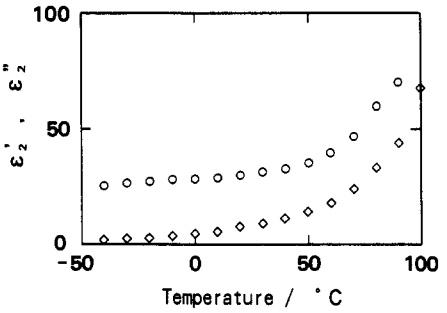

Figure 13. Temperature dependences of the real part of the dielectric constant, ϵ_2' (○), and of the imaginary part of ϵ_2'' (◇) for the PPP particle.

Temperature Dependence. Figure 12 indicates temperature dependence of G' and of tan δ under electric fields of 0 and 3 kV/mm. The horizontal axis in Figure 12 denotes the temperature in a chamber of the viscoelastic spectrometer. The polymer blend has a glass transition temperature of about −45 °C. As shown in Figure 12, the electroviscoelastic effect is observed in the rubbery state. The blend in the glassy state does not produce the electroviscoelastic effect because the effect may probably be too small. The changes of G' and of tan δ induced by an electric field of 3 kV/mm depend on temperature. The electroviscoelastic effect accelerates exceedingly over 50 °C, but it reaches a maximum at 110 °C. The real and imaginary parts of the dielectric constant of PPP particle no. 4 are plotted as functions of temperature in Figure 13. Both ϵ_2' and ϵ_2'' increase with temperature above 50 °C. The value of ϵ_2' is far more than 100 at 100 °C, while that of the silicone elastomer is about 3. This means that the electroviscoelastic effect becomes constant since $\kappa^2 \rightarrow 1$. In comparison with the data in Figures 12 and 13, the temperature dependence of the electroviscoelastic behavior is explained qualitatively by the point–dipole approximation model.

Field Intensity Dependence. According to the point–dipole approximation model, the amount of the electroviscoelastic effect is proportional to E^2. In Figure 14, the increments of the storage modulus by electric fields, $\Delta G'$ ($=G'(E) - G'(0)$), are plotted as functions of the intensity

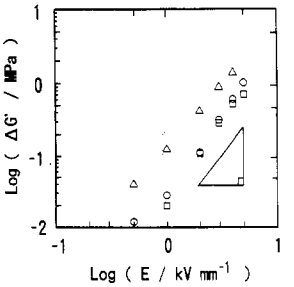

Figure 14. Field intensity dependences of G' at various temperatures: (○) −40 °C, (□) +25 °C, and (△) + 100 °C.

of applied fields. Figure 14 indicates the data at −40, +25, and +100 °C. $\Delta G'$ shows a quadratic dependence on the field intensity at each temperature.

5. Conclusion

In this paper, we presented experimental results on the electroviscoelastic effect of immiscible polymer blends composed of silicone elastomer and PPP particles doped with $CuCl_2$ or $FeCl_3$. We analyzed experimental results, especially the effects of the dielectric constant of the particle using the point–dipole approximation. The electroviscoelastic effect for the semiconducting polymer particle systems was based on microscopic interactions between electrically polarized particles. The present experiments have provided useful results for the understanding of the electroviscoelastic effect. It is expected to use electric fields to control the adhesion between dispersed phases in an immiscible polymer blend.

References and Notes

(1) Moriya, S.; Adachi, K.; Kotaka, T. *Polym. Commun.* **1985**, *26*, 235.
(2) Serpico, J. M.; Wnek, G. E.; Krause, S.; Smith, T. W.; Luca, D. J.; Van Laeken, A. *Macromolecules* **1991**, *24*, 6879.
(3) Venugopal, G.; Krause, S. *Macromolecules* **1992**, *25*, 4626.
(4) Serpico, J. M.; Wnek, G. E.; Krause, S.; Smith, T. W.; Luca, D. J.; Van Laeken, A. *Macromolecules* **1992**, *25*, 6373.
(5) Uejima, H. *Jpn. Appl. Phys.* **1972**, *11*, 319.
(6) Stangloom, J. E. *Phys. Technol.* **1983**, *14*, 290.
(7) Klass, D. L.; Martinek, T. W. *J. Appl. Phys.* **1967**, *38*, 67.
(8) Block, H.; Kelly, J. P.; Watson, T. *Spec. Publ. R. Soc. Chem.* **1991**, *87*, 151.
(9) Shiga, T.; Ohta, T.; Hirose, Y.; Okada, A.; Kurauchi, T. *Kobunshi Ronbunshu* **1990**, *48*, 47.
(10) Skotheim, T. A. *Handbook of Conducting Polymers*; Marcel Dekker, Inc.: New York, 1986; Vol. 1.
(11) Klingenberg, D. J.; van Swol, F.; Zukoski, C. F. *J. Chem. Phys.* **1989**, *91*, 7888.
(12) Klingenberg, D. J.; van Swol, F.; Zukoski, C. F. *J. Chem. Phys.* **1991**, *94*, 6160.
(13) Klingenberg, D. J.; van Swol, F.; Zukoski, C. F. *J. Chem. Phys.* **1991**, *94*, 6170.
(14) Whittle, M. *J. Non-Newtonian Fluid Mech.* **1990**, *37*, 233.
(15) Davis, L. C. *Appl. Phys. Lett.* **1992**, *60*, 319.
(16) Shiga, T.; Ohta, T.; Hirose, Y.; Okada, A.; Kurauchi, T. *J. Mater. Sci.* **1993**, *28*, 1293.
(17) Davis, M. H. *Quart. J. Mech. Appl. Math.* **1964**, *17*, 499.
(18) Kovacic, P.; Kyrlokis, A. *J. Am. Chem. Soc.* **1963**, *85*, 454.